

Design and Performance Test of the Soft Pneumatic Finger with Two Kinds of Air Cavities

Yan Zhang¹, Hongjie Zhang^{1,*} and Qi Zhang²

¹School of Mechanical Engineering, Tiangong University, Tianjin 300387, China

²Hangzhou Xiaoshan Technician College, Hangzhou 311200, China

*Corresponding author e-mail: zhanghj022@qq.com

ABSTRACT. To solve the problem of insufficient flexibility of the soft hand, this research proposes a new type of soft finger which consists of two kinds of air cavities. In this research, firstly, the structure of the newly proposed soft finger was determined, in which the root part of the finger adopts a series of low-speed deformation air cavities while the tip part of the finger adopts several fast-speed deformation air cavities. Secondly, the effects of the finger's geometries on the deformation performance were studied based on the Abaqus, then the geometric parameters were selected. Finally, an ARM microcontroller-based system was developed to test the performance of the soft finger, and the test results were compared with those from the finite element analysis. The error analysis between the finite element analysis and the experimental test proves the effectiveness of the design method, laying a solid foundation for the application of the newly proposed soft finger.

KEYWORDS: soft robots, soft fingers, finger with two air cavities, mould pouring

1. Introduction

As one of the important end effectors, the manipulator plays an irreplaceable role in our production and life. As shown in Figure.1, traditional mechanical manipulators are usually composed of rigid structures, which are mostly driven by various of motors. Although the traditional manipulator has many advantages, such as large output force, large carrying capacity and high control accuracy, it is difficult to grasp fragile and irregular objects due to rigid contact and insufficient

flexibility.



Figure. 1

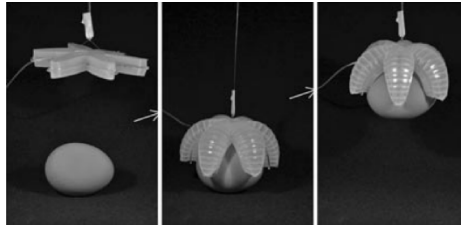


Figure. 2

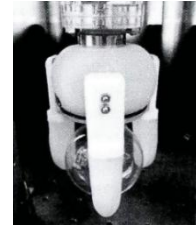


Figure. 3

In recent years, with the rise of new materials and scholars' research on bionics, soft manipulators have attracted attention. The design inspiration for soft manipulators usually comes from soft creatures, such as octopus [1] and worms [2]. Soft manipulators are usually composed of a certain number of soft fingers and are driven by air pressure, because pneumatic drives have the advantages of easy access to raw materials, fast response speed and low cost. They have flexible contact with external objects and can change their shape according to the objects they grab, and have great potential for application in the fields of medicine and rescue [3].

At present, scholars at home and abroad have proposed a variety of soft pneumatic grippers. As shown in Figure.2, Harvard University Ilievski et al. proposed a sea star-like soft gripper adopting a pneumatic grid structure [4], which can grab fragile objects. Beihang University has developed a four-finger pneumatic gripper, which can easily grasp objects such as eggs and bagged milk [5]; As shown in Figure.3, Xu Miaoxin of Nanjing University of Science and Technology designed a pneumatic soft claw with three tentacles [6], and studied the driving model of the claw. The WALSH group uses fibers to control the deformation of the fingers, and develops soft hands that can assist patients with special hand training [7-8]. Although these soft manipulators have good flexibility, but their fingers are mostly single-air cavity structure, the flexibility is insufficient, and the range of motion is limited.

In view of the above problems, it is very necessary to improve the flexibility of the manipulators, therefore, through appropriate improvements to the structure of

existing fingers, this investigation proposed a new type of soft finger with two air cavities, which combines slow PneuNet and fast PneuNet structures. This finger has a certain grasping force on the basis of flexible deformation. In addition, the finite element simulation and experimental test were carried out on the deformation performance of the proposed pneumatic finger, which verified the rationality of the design.

2. Working principle and structure design of pneumatic soft finger

2.1 Working principle

The newly designed soft finger used the PneuNet structure proposed by Harvard University [9]. A group of schematic diagrams for this structure frequently used are shown in Figure.4, where (a) is fast PneuNet (FPN), and (b) slow PneuNet (SPN). Extensible layer and strain limiting layer are the two basic components of the PneuNet structure, among which the extensible layer involves some interconnected airbags, together with the strain limiting layer, a closed cavity is constituted. Commonly, the soft finger is pneumatically-driven. When the air pressure increases, the airbags will expand. Under the action of the strain limiting layer, the deformation of the extensible layer is limited. This differential strain causes the finger to bend. Compared with the SPN, the FPN deforms comparatively faster, but it is only able to withstand a small pressure, inversely, the SPN structure deforms slowly, but can bear a comparatively bigger pressure.

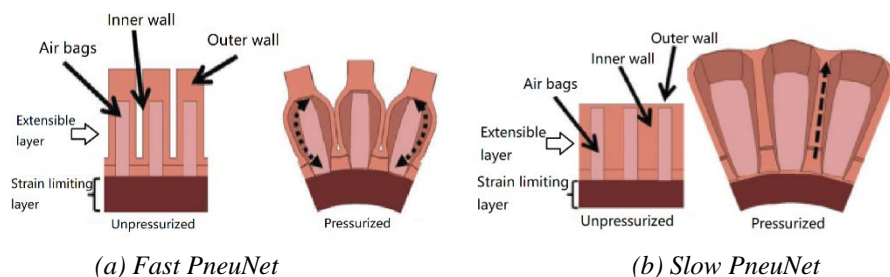


Figure. 4 Schematic diagram for the PneuNet structure

2.2 Structure design of the finger

Figure.5 shows the three-dimensional model of the newly designed soft finger and it consists of SPN and FPN structure. The root and middle part of the finger adopts SPN structure, while the tip part of the finger adopts the FPN structure. Thus, the advantages of the SPN and FPN structure can be combined in one soft finger, that is to say, the newly proposed soft finger possesses better flexibility and rigidity.

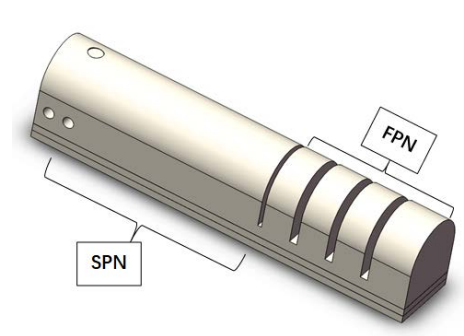


Figure. 5 The structure of the soft pneumatic finger with two air cavities

3. The influence of geometric parameters on the deformation of the finger

To analyze the effect of the geometric parameters on the deformation ability of the finger, and to select the optimal sizes, the finite element analysis was performed based on the Abaqus software. In order to improve the analysis efficiency, the models of the double airbag structure is established for analysis. One end of the double airbag model is fixed, and its deformation performance is expressed by the displacement of the other end. As shown in Figure.6, there are several key geometries in these basic constitutions of the soft pneumatically-driven fingers. As listed in Table.1, the geometries include cross-sectional shape, inner wall thickness, outer wall thickness, space between two airbags, airbag length. In Figure.7, finite element models of the double airbag structure of FPN and SPN are established. Traditionally, the Yeoh model is widely used to represent the material properties of the superelastic material [10-11]. These models are divided through tetrahedral mesh. To evaluate the deformation abilities of these two types of double airbag

structure, the displacement of one end of the model versus a gradually increased air pressure is measured. Figure.7(a) shows the deformation of the FPN under the pressure of 40kPa and the Figure.7(b) displays the deformation of the SPN under the pressure of 80kPa.

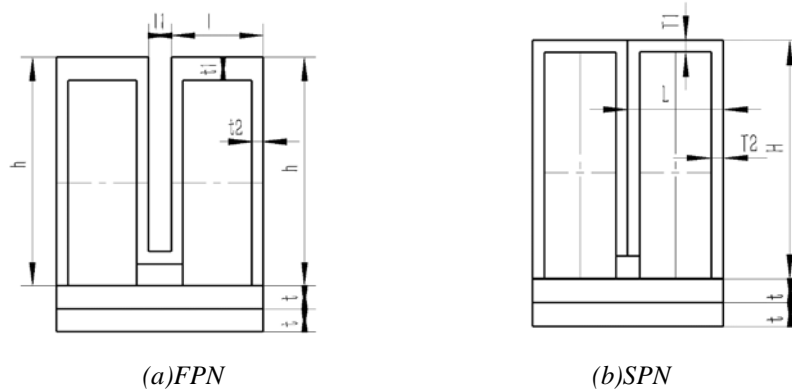


Figure. 6 Finite element models of double airbag structures

Table 1 Symbols and meanings of geometric parameters

Symbol	Parameter
l	Airbag length of FPN
l_1	Space between two airbags of FPN
t_1	Outer wall thickness of FPN
t_2	Inner wall thickness of FPN
h	Airbag height of FPN
L	Airbag length of SPN
T_1	Outer wall thickness of SPN
T_2	Inner wall thickness of SPN
H	Airbag height of SPN
t	Half the thickness of the bottom layer

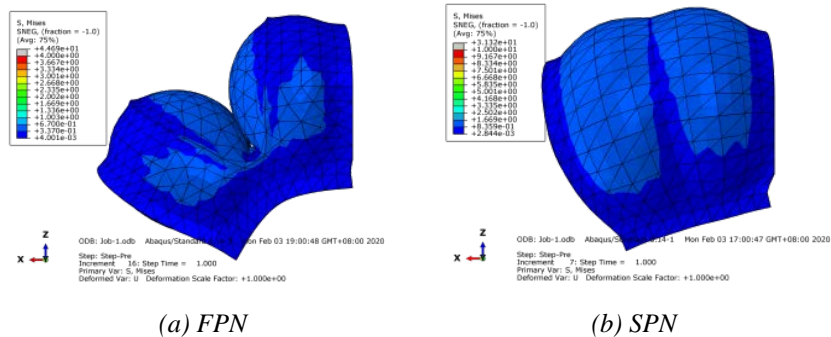


Figure. 7 Finite element models of double airbag structures

For the SPN structure, the effect of the cross-sectional shape on the deformation ability is investigated first. Commonly, there are two basic shapes, i.e. the rectangular cross-section and D-shaped cross-section. The results are shown in Figure.8(a) where the pressure increases from 0 to 80 kPa. It can be found that the deformation of the D-shaped cross-section is slightly larger than that of the rectangular cross-section, presenting slightly better flexibility. Then, the influence of the outer wall thickness is observed. As shown in Figure.8(b) in which four types of thickness are considered and they are 0.5, 1.0, 1.5, and 2.0 mm, it can be seen that the deformation of the airbag increases approximately linearly with the increase in the pressure. In the meanwhile, deformation ability of the airbag is enhanced with the decrease in the outer wall thickness, it is to say, the smaller the thickness of the outer wall, the greater the degree of deformation.

For the FPN structure, the effect of the cross-sectional shape on the deformation ability is investigated. The results are shown in Figure.9(a) where the pressure increases from 0 to 40 kPa. It can be found that the deformation of the rectangular cross-section is slightly larger than that of the D-shaped cross-section, presenting slightly better flexibility, but the maximum stress value of the deformation of the D-shaped cross-section is slightly smaller than that of the rectangular cross-section. And the consistency of the cross-sectional shape with that of SPN is considered, so the D-shaped cross-section is selected. Then, the influence of the inner wall thickness, space between two airbags and outer wall thickness is observed. As shown in Figure.9(b) in which four types of inner wall thickness are considered and

they are 0.5, 1.0, 1.5, and 2.0 mm, it can be seen that the deformation of the airbag increases approximately linearly with the increase in the pressure. At the same time, deformation ability of the airbag is enhanced with the decrease in the inner wall thickness, it is to say, the smaller the thickness of the inner wall, the greater the degree of deformation. As can be seen from Figure.9(c), where three types of space between two airbags are considered and they are 1.0, 2.0, and 3.0 mm, it can be seen that the deformation of the airbag increases approximately linearly with the increase in the pressure. Meanwhile, deformation ability of the airbag is enhanced with the decrease in the space, it is to say, the smaller the space between two airbags, the greater the degree of deformation, but too small space will cause stress to be too concentrated. As shown in Figure.9(d) in which three types of outer wall thickness are considered and they are 1.0, 2.0 and 3.0 mm, it can be seen that the deformation of the airbag increases approximately linearly with the increase in the pressure. Meantime, deformation ability of the airbag is enhanced with the decrease in the outer wall thickness, that is to say, the smaller the thickness of the outer wall, the greater the degree of deformation.

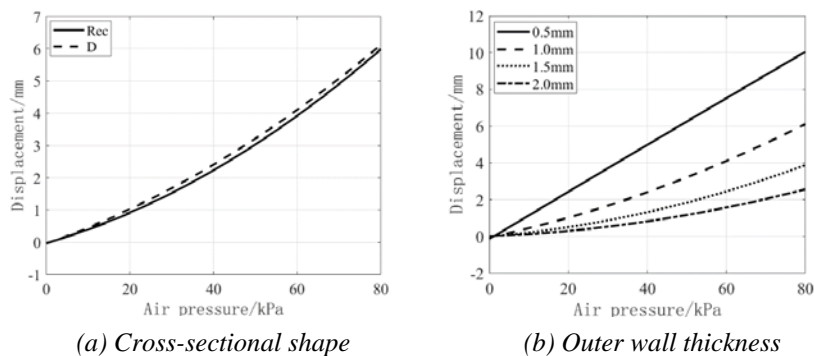


Figure. 8 The influence of structural parameters on the deformation effect of the first air cavity

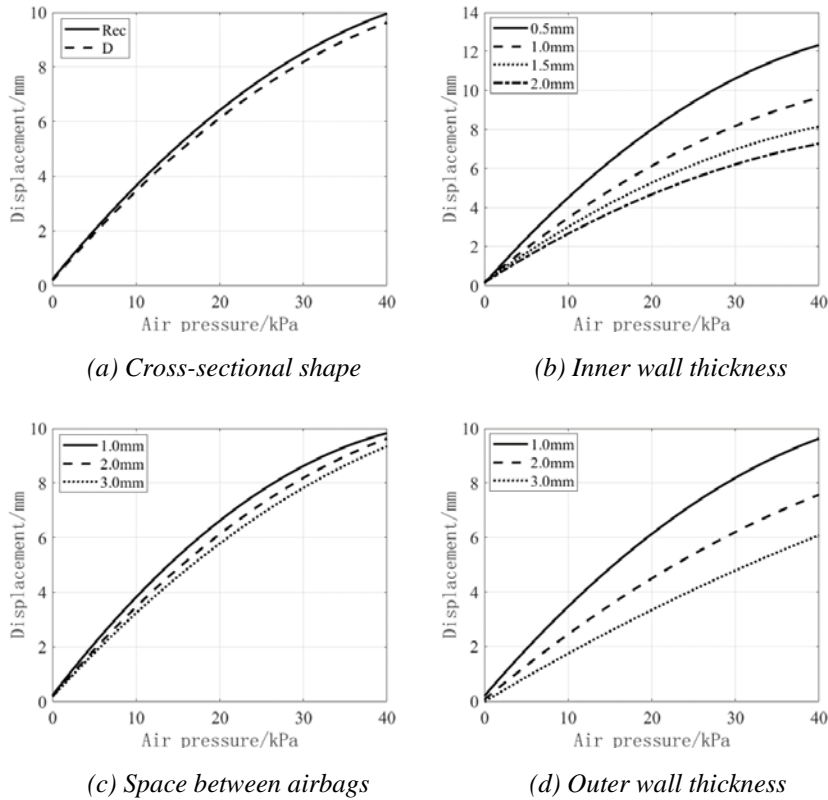


Figure. 9 The influence of structural parameters on the deformation effect of the second air cavity

In order to analyze the effect of the number of airbags (or the airbag length) on the deformation ability of the finger, in Figure.10, finite element models with different numbers of airbags for the same total length are established. One end of these models is fixed, and the deformation performance is expressed by the overall bending angle. As shown in Figure.11(a), in which three types of number of airbags for SPN are considered and they are 8, 5, and 4, it can be seen that the deformation of the model increases approximately linearly with the increase in the pressure. In the meanwhile, deformation ability of the model is almost the same with the changes of the number of airbags for SPN. As can be seen from Figure.11(b), where three types of number of airbags for FPN are considered and they are 6, 4,

and 3, it can be seen that the deformation of the model increases with the increase in the pressure. At the same time, deformation ability of the model is enhanced with the increase in the number of airbags for FPN, it is to say, the more the number of airbags, the greater the degree of deformation for FPN.

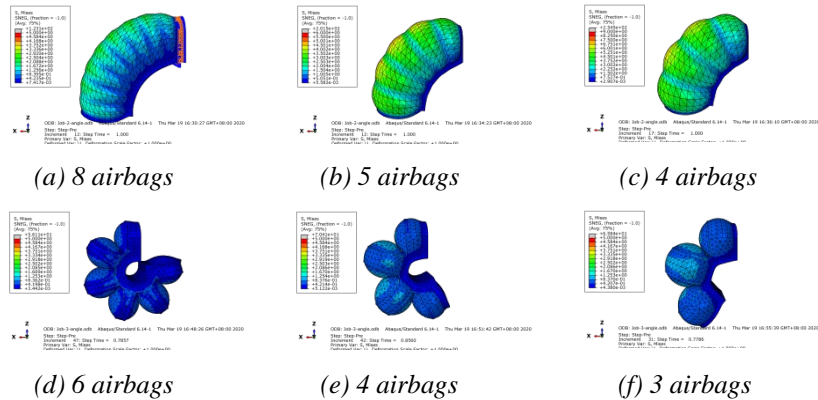


Figure. 10 Finite element models with different number of airbags when the total length is unchanged

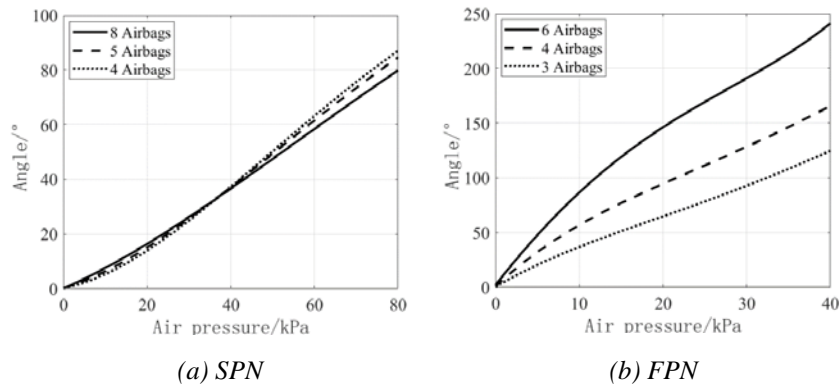


Figure. 11 The influence of the number of airbags on the deformation effect

Based on the above analysis, the geometric parameters of the soft finger are finally determined, as listed in Table.2.

Table 2 Geometric parameters of the soft pneumatic finger

Parameter	Size/(mm)
Total length	105
Outer wall thickness of the SPN	1
Single airbag length of the SPN	5
Outer wall thickness of the FPN	2
Inner wall thickness of the FPN	1
Space between airbags of the FPN	2
Single airbag length of the FPN	8

4. Performance test of finger prototype

4.1 Construction of the experimental platform

To investigate the flexibility of the newly proposed soft finger and test the effectiveness of the used design method, the soft finger was made of silicone rubber material and a prototype photo of the finger is shown in Figure.12. Then an experimental system was built. The experimental system includes a pneumatic drive unit, a circuit control unit, and a data acquisition unit. The air pump (OTS-550) is used as a gas source. After being processed by the gas source processor, the high-pressure gas passes through a pressure regulating valve whose output can change from 0 to 600 kPa when its control voltage varies from 0 to 10 V. Here, a self-developed embedded control system based on ARM microcontroller was used to regulate the control voltage level of the valve.

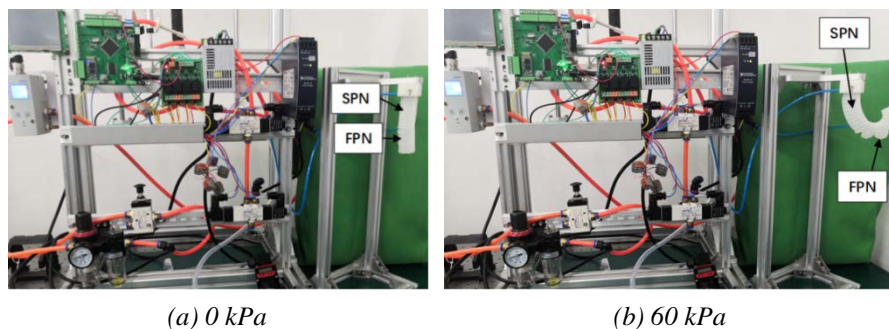
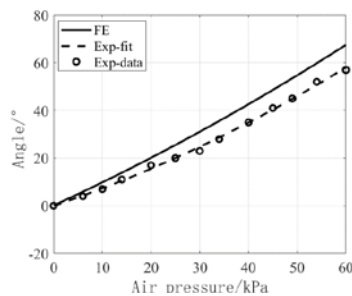


Figure. 12 Experimental system

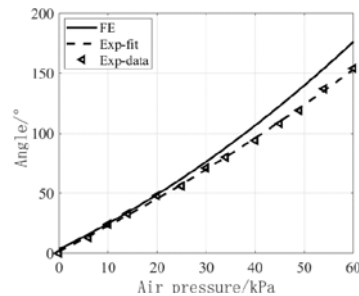
4.2 Performance testing of the finger

To test the performance, the SPN and FPN of the soft finger are fed with the same air pressure. In this test, the air pressure increased from 0kPa to 60kPa with 5kPa of interval. and the photos of the bended finger under the different air pressures are taken by the camera. Then, the bend angle was measured by the picture processing. Figure.12 shows the experimental scenes where (a) corresponds to the pressure of 0kPa, while (b) to 60kPa.

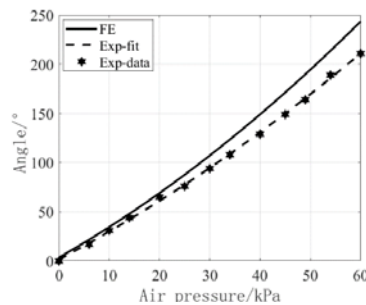
As can be seen from the curves of bend angle regarding pressure in Figure.13, the deformation of the soft finger increases approximately linearly with the increase in the pressure. In the meanwhile, the deformation results of the finite element analysis are slightly lower than those of the experiment, and the error increases as the increase of air pressure. This error is due to the insufficient manufacturing accuracy of the soft finger, which makes the bottom too thick, resulting in a large bending resistance. This test manifests the rationality of the designed method on the soft finger.



(a) Bending angle of the first cavity



(b) Bending angle of the second cavity



(c) Total bending angle

Figure. 13 Comparison of bending angle between experiment and finite element

5. Conclusion

This study proposes a new type of soft finger that can be used in the applications of soft robotics. The finger combines the characters of the SPN-based soft finger and the FPN-based one. To finish the design of this new type soft finger, the main geometric parameters that affect the deformation of the finger are analyzed based on the Abaqus, and the performance of the prototype was tested by ARM microcontroller-based system. The tested results verified the effectiveness of the finite element analysis, proving the rationality of the design, and provide a basis for further research and application on soft fingers.

References

- [1] Margheri L, Laschi C, Mazzolai B. Soft robotic arm inspired by the octopus: I. From biological functions to artificial requirements [J]. *Bioinspiration & Biomimetics*, 2012, 7 (2): 1-12.
- [2] Seok S, Onal C D, Cho K J, et al. Meshworm: a peristaltic soft robot with antagonistic nickel titanium coil actuators [J]. *IEEE/ASME Transactions on Mechatronics*, 2012, 18 (5): 1485.
- [3] LI Tiefeng, LI Guorui, LIANG Yiming, et al. Review of Materials and Structures in Soft Robotics [J]. *Chinese Journal of Theoretical and Applied Mechanics*, 2016, 48 (04): 756-766.
- [4] Ilievski F, Mazzeo A D, Shepherd R F, et al. Soft Robotics for Chemists [J]. *Angewandte Chemie*, 2011, 50 (8): 1890-1895.
- [5] Hao Y F, Gong Z Y, Xie Z X, et al. Universal soft pneumatic robotic gripper with variable effective length [C] //35th Chinese Control Conference (CCC). 2016: 6109-6114.
- [6] Xu Miaoxin, Li Xiaoning, Guo Zhonghua. Study of Mathematical Model of Soft Finger in New Flexible Gripper [J]. *Machine Building & Automation*, 2016, 45 (5): 99-102.
- [7] Polygerinos P, Galloway K C, Savage E, et al. Soft robotic glove for hand rehabilitation and task specific training [C]// IEEE International Conference on Robotics and Automation, 2015: 2913-2919.
- [8] Polygerinos P, Wang Z, Galloway K C, et al. Soft robotic glove for combined assistance and at-home rehabilitation [J]. *Robotics and Autonomous Systems*, 2015, 73: 135-143.
- [9] Mosadegh B, Polygerinos P, Keplinger C, et al. Soft Robotics: Pneumatic Networks for Soft Robotics that Actuate Rapidly [J]. *Advanced Functional Materials*, 2014, 24 (15): 2163-2170.

- [10] Huang Jianlong, Xie Guangjuan, Liu Zhengwei. FEA of Hyperelastic Rubber Material Based on Mooney-Rivlin Model and Yeoh Model [J]. China Rubber Industry, 2008 (08): 467-471.
- [11] Zheng Mingjun, Wang Wenjing, Chen Zhengnan, et al. Determination for Mechanical Constants of Rubber Mooney-Rivlin Model [J]. China Rubber Industry, 2003 (08): 462-465.